Analytical Bearing Capacity of Strip Footings in Weightless Materials with Power-Law Failure Criteria

Alcibiades Serrano; Claudio Olalla; and Rafael Jimenez

Abstract: Sokolovskii's method of characteristics is extended to provide analytical solutions for the ultimate load at the moment of plastic failure under plane-strain conditions of shallow strip foundations on weightless rigid-plastic media with a noncohesive power-law failure envelope. The formulation is made parametrically in terms of the instantaneous friction angle, and the key idea to obtain the bearing capacity is that information can be transmitted from the free surface (where external loads are known) to the contact plane of the foundation. The methodology can consider foundations adjacent to a slope, external surcharges at the free surface, and inclined loads (both on the slope and on the foundation). Sensitivity analyses illustrate the influence on bearing capacity of changes in the different geometrical parameters involved. An application example is presented and design plots are provided, and model predictions are compared with results of bearing capacity tests under low gravity.

Author keywords: Plastic failure; Characteristics lines; Sokolovskii's method; Nonlinear failure envelope; Toyoura sand.

Introduction

Closed-form bearing capacity solutions for shallow foundations on materials with a linear failure criterion have been obtained using limit equilibrium and plasticity theory. For instance, building on work by Prandtl in 1920, Terzaghi (1943) proposed his bearing capacity formula with three independent terms (i.e., external surcharge, cohesion, and soil's self-weight); the formula was later extended to consider shape, depth, and load inclination factors, among other corrections (e.g., Meyerhof 1951; Brinch-Hansen 1961; Vesic 1975).

Limit analysis (Chen 1975) has also been employed to compute bearing capacity. The upper-bound theorem states that any kinetically admissible failure mechanism produces an upper bound to the failure load; due to the simplicity of its energy approach, it has been more widely used (e.g., Baker and Frydman 1983; Drescher and Detournay 1993; Michalowski 1997; Ukritchon et al. 1998). Improved upper-bound and lower-bound solutions have been obtained by integrating limit analysis, finite-element analysis, and nonlinear programming (e.g., Lyamin and Sloan 2002a, b; Kumar and Khatri 2008).

The characteristic (or slip lines) method has also been employed to compute the bearing capacity of shallow foundations; for example, Sokolovskii (1965) obtained complete numerical solutions for rigid-plastic materials with a linear failure criterion. Similarly, Pope (1975) solved Sokolovskii's equations numerically to develop simplified bearing capacity charts for shallow foundations; Ko and Scott (1973) used stress fields computed using Sokolovskii's characteristics method to determine the failure conditions of shallow footings; and Bolton and Lau (1993) used the method of characteristics to compute bearing capacity factors for circular and strip shallow footings on $c-\phi$ soils. The method has also been extended to rigid-plastic materials with nonlinear failure criteria (Sokolovskii 1965; Serrano 1976; Graham and Hovan 1986; Ueno et al. 2001; Zhu et al. 2001; Lau and Bolton 2011; Spasojevic and Cabarkapa 2012) and to materials obeying the Hoek–Brown failure criterion (Serrano and Olalla 1994).

Although many contributions indicated above consider linear Mohr–Coulomb (MC) failure envelopes, failure envelopes for soils are commonly curved (e.g., Bishop 1966; Baker 2004; Serrano and Olalla 2006), with (except for cemented soils) a very small or negligible cohesion intercept (Mitchell and Soga 2005). Experimental results also suggest cohesionless nonlinear strength envelopes for rockfill materials (e.g., Charles and Watts 1980; Indraratna et al. 1993), as well as for many other soil types (e.g., Bolton 1986; Maksimovic 1989, 1996; Maeda and Miura 1999).

Building on recent research on power-type failure criteria for geomaterials (see Anyaegbunam 2013, who provides a numerical method for evaluating the earth pressures on smooth retaining walls under plane strain conditions for this type of failure criteria), the authors extend Sokolovskii's method of characteristics to derive simple analytical solutions to compute the bearing capacity, under plane-strain conditions and for a uniform surcharge (traction), of weightless rigid-plastic media with a noncohesive power-law failure envelope. (Note that this definition of bearing capacity is applicable to flexible foundations or uniform surcharges; hence, it is slightly different from the traditional geotechnical definition, in which average tractions are computed at the interface of the soil with the foundation, without consideration of the actual distribution of stresses at the interface.) Because analytical (or closed-form) solutions are not available for the characteristics method and materials with weight (Lau and Bolton 2011; Spasojevic and Cabarkapa 2012), the authors needed to assume a weightless material. However, neglecting the soil's self weight might be overly conservative for noncohesive soils and, in particular, for large

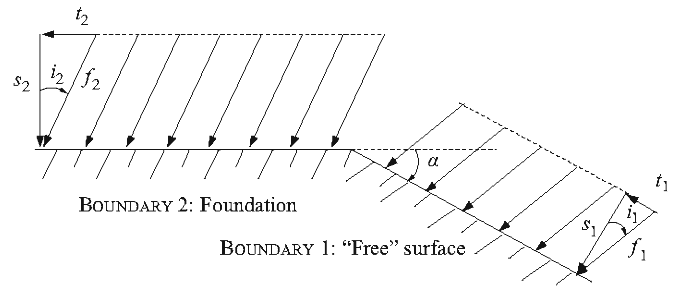

Fig. 1. Foundation model and (positive) sign criterion for angles of inclined loads

foundations with rough interfaces; therefore, the authors discuss, in the context of previous research on bearing capacity with nonlinear failure criteria (e.g., Ueno et al. 2001; Spasojevic and Cabarkapa 2012; Zhu et al. 2001; Lau and Bolton 2011; Kumar and Khatri 2008; Graham and Hovan 1986), how to estimate the contribution of the soil's unit weight on bearing capacity in real cases.

Fig. 1 illustrates the foundation model considered, as well as the sign criteria employed for the slope and the inclined loads. The methodology allows foundations adjacent to a slope, external surcharges at the free surface, and inclined loads (both on the slope and on the foundation). Its use is illustrated with a worked example that also serves to conduct sensitivity analyses, and it is also employed to verify the results of recent bearing capacity tests conducted under low-gravity conditions (Kobayashi et al. 2007, 2009). Finally, design graphs that allow quick and approximate computations without having to implement all expressions provided are presented.

Failure Criterion

Definition and Normalization

The authors work with noncohesive weightless materials with a nonlinear failure criterion given by the following (power-law) equation:

$$\tau = A \cdot \sigma^n \tag{1}$$

where $\tau =$ shear strength on such a plane; $\sigma =$ effective normal stress at the failure plane; and n is an exponent with value $1/2 < n < 1$ [see below, and the discussion in Anyaegbunam (2013), for details] that defines the shape of the envelope.

Because it is convenient to work with normalized (i.e., dimensionless) variables, a normalizing stress parameter was defined, β_0, given by the effective normal stress at the intersection between the failure criterion and a 1:1 slope auxiliary line in the Mohr (σ, τ) space (see Fig. 2). Using $A = \beta_0^{(1-n)}$,

$$\tau^* = (\sigma^*)^n \tag{2}$$

is obtained where the notations $\sigma^* = \sigma/\beta_0$ and $\tau^* = \tau/\beta_0$ have been used.

Instantaneous Friction Angle

The friction angle of materials with a nonlinear failure criterion is not constant. Using Mohr's envelope as the failure criterion, $\tau = \tau(\sigma)$, the instantaneous friction angle, ρ, can be defined as

$$\frac{d\tau}{d\sigma} = \tan \rho = n(\sigma^*)^{n-1} \tag{3}$$

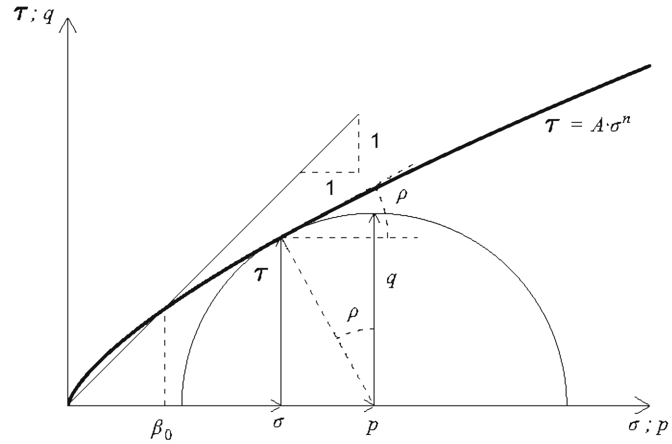

Fig. 2. Definition of β_0 and ρ and their relationship with the power-law failure criterion

The instantaneous friction angle allows parametric formulations of the failure criterion. For instance, from Eqs. (1) and (3)

$$\sigma = \beta_0 \left(\frac{n}{\tan \rho} \right)^{\frac{1}{1-n}} \tag{4}$$

$$\tau = \frac{\sigma}{n} \tan \rho \tag{5}$$

As a cautionary remark, the reader should note that the power-law assumption could lead to very high friction angles for applications involving low stress levels, so that other types of nonlinear failure criteria (e.g., Graham and Hovan 1986; Maksimovic 1996, 1989; Bolton 1986) might be more adequate in such cases. However, because stress levels below a foundation at failure are expected to be high, this will not be very relevant in bearing capacity applications—especially when there is a surcharge on the external boundary.

The failure criterion can also be expressed using Lambe's variables, $p = (\sigma_I + \sigma_{III})/2$ and $q = (\sigma_I - \sigma_{III})/2$, where σ_I and σ_{III} are, respectively, the major and minor principal stresses. For associated plastic flow with coaxial plasticity, Lambe's variables (p, q) are related to the stresses at the failure plane (σ, τ) by (see Fig. 2)

$$q = \frac{\tau}{\cos \rho} \tag{6}$$

$$p = \sigma + \tau \tan \rho = \sigma + q \sin \rho \tag{7}$$

and, using Eqs. (3), (6) and (7), the instantaneous friction angle becomes (Serrano and Olalla 1994)

$$\frac{dq}{dp} = \sin \rho \tag{8}$$

Similarly, the power-law failure criterion [Eq. (1)] yields the following parametric equations for Lambe's variables:

$$q = \frac{\sigma}{n} \frac{\sin \rho}{\cos^2 \rho} \tag{9}$$

$$p = \sigma \frac{n + (1-n)\sin^2 \rho}{n \cos^2 \rho} \tag{10}$$

which results in

$$\frac{p}{q} = \frac{n + (1-n)\sin^2 \rho}{\sin \rho} \tag{11}$$

Resolution of the System by the Method of Characteristics

Introduction

The method of characteristics (Sokolovskii 1965) can solve the hyperbolic system of partial differential equations that characterize the stress state, under plane-strain conditions, of rigid-plastic media with a Coulomb-type failure criterion. Serrano (1976) showed that Sokolovskii's method could be extended to materials with nonlinear failure criteria of the MC type [i.e., expressed as $q = q(p)$], as long as the system of partial differential equations is hyperbolic. Such hyperbolicity condition is given by

$$\left|\frac{dq}{dp}\right| \leq 1 \tag{12}$$

which is, of course, equivalent to ρ being real [see Eq. (8)].

In addition, for associated plasticity and the power-law failure criterion considered herein, it can be demonstrated that Eq. (12) holds as long as $1/2 \leq n$. Note, however, that there is the additional restriction that $n \neq 1/2$ to avoid having a nonzero uniaxial compressive strength with an otherwise cohesionless material (Graham and Hovan 1986; Serrano and Olalla 2006); such conditions limit the validity of our solutions to the range $1/2 < n < 1$ as feasible n values. The limiting case of $n = 1$ corresponds to a linear failure criterion, in which case our results converge to Prandtl's solution; see the Appendix. For the range of admissible n values with failure criteria of the type $\tau = (A + B\sigma)^n$, see Anyaegbunam (2013).

Method of Characteristics

The differential equations of the two families of characteristic lines are

$$\frac{dy}{dx} = \tan(\psi \pm \mu) \tag{13}$$

where $\mu = \pi/4 - \rho/2$, $\psi =$ angle that the major principal stress forms with the vertical axis x, and $\rho =$ instantaneous friction angle. The positive sign of Eq. (13) defines the α characteristic lines, whereas the negative sign defines the β characteristic lines (see Fig. 3).

In addition to the characteristic lines defined by Eq. (13), it is also verified that (Serrano 1976)

$$dI \pm d\psi = \mp \frac{W_X \sin(\psi \mp \mu) - W_Y \cos(\psi \mp \mu)}{2q\cos(\psi \pm \mu)} dx \tag{14}$$

where

$$dI = \frac{\cos\rho}{2q} dp \tag{15}$$

is the differential of Riemann's invariant, and where W_X and W_Y are the vertical and horizontal components of the mass forces acting on the soil element. For instance, if the self-weight is the only body force acting on the soil mass, then $W_X = \gamma$ ($\gamma =$ unit weight of the material) and $W_Y = 0$. Alternatively, if there are no mass forces (for the case of a weightless material), $W_X = W_Y = 0$ and Eq. (14) becomes

$$dI \pm d\psi = 0 \tag{16}$$

where the plus sign corresponds to the α family of characteristic lines and the minus sign corresponds to the β family.

Assuming that there is a singularity at the corner between Boundaries 1 and 2, from where a series of characteristics leave the corner with different inclinations (Graham and Hovan 1986), and integrating Eq. (16) along the α family of characteristic lines (i.e., using the plus sign) from the source given by the boundary outside the foundation (Boundary 1; see Fig. 1), and toward the target given by the boundary where the foundation load is applied (Boundary 2),

$$I(\rho_1) + \psi_1 = I(\rho_2) + \psi_2 \tag{17}$$

where $I(\rho)$ is (somewhat loosely) referred to as Riemann's invariant.

Multiplying and dividing by p in Eq. (15), the following is obtained:

$$dI = \frac{\cos\rho}{2}\left(\frac{p}{q}\right)\left(\frac{dp}{p}\right) \tag{18}$$

Further, using the failure criterion relationships in Lambe's variables [Eqs. (9) and (10)], results in

$$dI = \frac{(n + (1-n)\sin^2\rho)}{2\tan\rho}\frac{d\sigma}{\sigma} + d\rho \tag{19}$$

which is the most general expression for the differential of Riemann's invariant.

Eqs. (17) and (19) are the key equations to obtain the bearing capacity (or, in other words, the ultimate load for plastic failure) for the foundation model when the material is weightless. To that end, information is transmitted from Boundary 1 to Boundary 2; that is, with the values of ψ_1 and ρ_1 at the exterior surface (Boundary 1, where the external loads are assumed known), it is possible to obtain the values of ψ_2 and ρ_2 below the foundation (i.e., on Boundary 2). Once that ρ_2 is known, the bearing capacity of the foundation, p_h can be computed, since it is only a function of ρ_2 and of the angle of (known) inclination of the foundation load i_2.

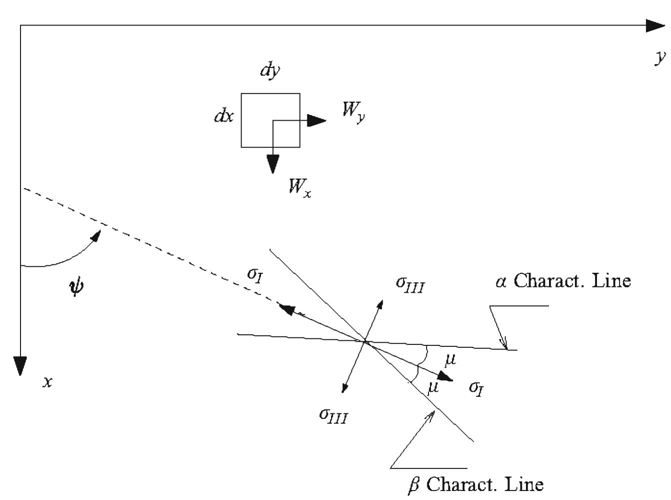

Fig. 3. Notation of variables involved in the differential equation of the families of characteristic lines

Computation of the Invariant

For the general case with $1/2 < n < 1$, differentiating Eqs. (4) and (5) gives

$$\frac{d\sigma}{\sigma} = -\frac{1}{(1-n)}\frac{\tan\rho}{\sin^2\rho}d\rho \tag{20}$$

from which

$$dI = \frac{1}{2}\left(1 - \frac{n}{(1-n)\sin^2\rho}\right)d\rho \tag{21}$$

and, integrating,

$$I = \frac{1}{2}\left(\rho + \frac{n}{(1-n)\tan\rho}\right) \tag{22}$$

which is the most general expression for the invariant.

Computing the Bearing Capacity

Description of the Procedure

Loads acting on the free surface of Boundary 1 (i.e., outside the foundation), as well as their inclination, are assumed to be known; that is, given the total external load f_1, its normal and tangential components are given, respectively, by $s_1 = f_1 \cos i_1$ and $t_1 = f_1 \sin i_1$, from which

$$t_1 = s_1 \tan i_1 \tag{23}$$

(Similar relations hold for f_2, s_2, t_2 and i_2 at Boundary 2 but, for brevity, they are not reproduced herein.)

To compute the loads on the foundation (Boundary 2) that produce plastic yield (i.e., bearing capacity failure), the following steps are needed (Serrano 1976; Serrano and Olalla 1994):

1. The stress state at Boundary 1 is defined by the normal stress s_1 and by the shear stress t_1. Such stress state corresponds to a single value of the instantaneous friction angle, ρ_1, for a given inclination, ψ_1, of the major principal stress (which is also related to the slope angle, α).
2. At Boundary 2, where the foundation load is acting, the relationship between the instantaneous friction angle, ρ_2, and the inclination of the major principal stress is given by Eq. (17), where Riemann's invariant is given by Eq. (22).
3. To obtain ρ_2, however, an additional equation relating ρ_2 and ψ_2 is needed. Such a condition may be given by the angle of incidence, i_2 of the foundation traction acting on Boundary 2.
4. The external load (traction) at Boundary 2 required to produce the plastic yield of the foundation, f_2, can be determined from the instantaneous friction angle ρ_2. With the angle of incidence of such load (i_2), its normal component can be used to compute the bearing capacity of the foundation, p_h, as $p_h \equiv s_2 = f_2 \cos i_2$.

Solution on the Free Surface (Boundary 1)

Instantaneous Friction Angle

To compute the instantaneous friction angle on Boundary 1 (see Step 1 above), the (known) stress state acting on it can be used. At failure, such stress state is on the corresponding Mohr's circle that is tangent to the failure envelope (see Fig. 2). Therefore, the following equation holds:

$$t_1^2 + (p_1 - s_1)^2 = q_1^2 \tag{24}$$

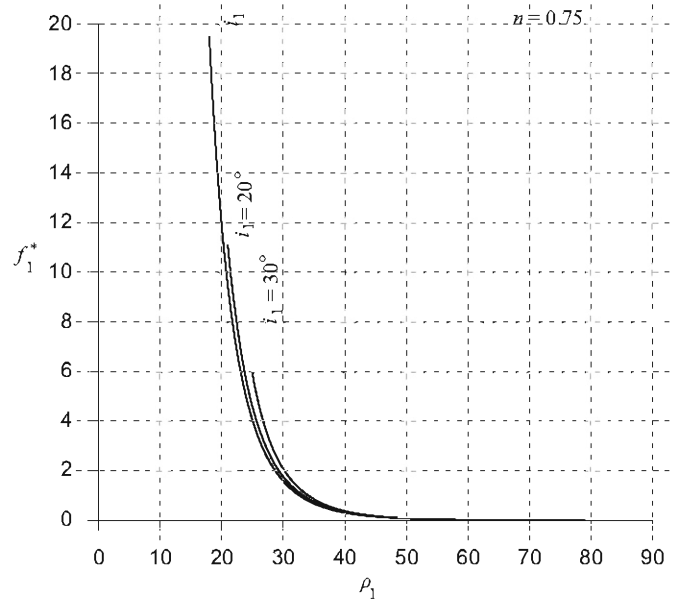

Fig. 4. Variation of the (normalized) external stress on the free surface as a function of ρ_1 and i_1 (for constant $n = 0.75$)

from which, using Eq. (23) and simplifying, it is obtained that

$$f_1 = \frac{s_1}{\cos i_1} = q_1\left(\frac{p_1}{q_1}\cos i_1 \pm \sqrt{1 - \left(\frac{p_1}{q_1}\right)^2 \sin^2 i_1}\right) \tag{25}$$

Substituting the power-law failure criterion [Eqs. (9) and (11)] into Eq. (25), and selecting the negative value of the square root,

$$f_1 = \beta_0\left(\frac{n}{\tan\rho_1}\right)^{\frac{1}{(1-n)}}\frac{\sin\rho_1}{n\cos^2\rho_1}\times \left[\left(\frac{n+(1-n)\sin^2\rho_1}{\sin\rho_1}\right)\cos i_1 - \sqrt{1-\left(\frac{n+(1-n)\sin^2\rho_1}{\sin\rho_1}\right)^2 \sin^2 i_1}\right] \tag{26}$$

Eq. (26) provides the instantaneous friction angle ρ_1 at the free surface (on Boundary 1) from the external traction f_1 (with inclination i_1) acting on it. As an illustration, Fig. 4 shows the nondimensional external traction ($f_1^* = f_1/\beta_0$) for a series of cases computed with $n = 0.75$ and for different values of i_1. (Note that i_1 has a limited influence on the results, which, as indicated below, is an interesting result from a practical perspective.)

Inclination of the Major Principal Stress

Following the notation above, ψ_1 indicates the angle of the major principal stress on Boundary 1 (i.e., on the free surface). Fig. 5 presents the Mohr's circle corresponding to the stress state at Boundary 1. The procedure to construct the Mohr's circle is as follows: (1) plot point T corresponding to the stress state at Boundary 1; (2) obtain the (passive) Mohr circle that passes through T and is tangent to the failure criterion; (3) because T acts on a plane forming an angle α with the horizontal, obtain pole; and (4) using the pole, obtain the plane on which σ_{III} acts. This plane forms angles ψ_1 with the vertical direction and ε_1 with the horizontal direction. It can be observed that ψ_1 can be obtained from angles ε and θ, so that $\psi_1 = \pi/2 + \varepsilon_1$, with $2\varepsilon_1 = \theta_1 - 2\alpha$, and with

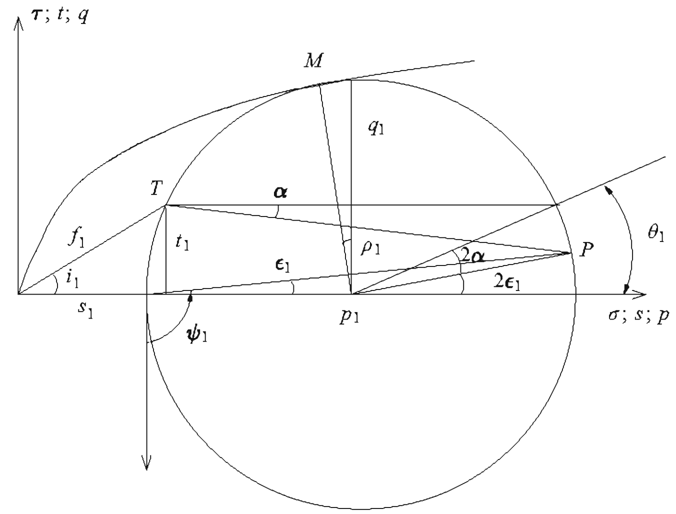

Fig. 5. Mohr's circle for the stress state at Boundary 1 (p = Pole; t = Traction on Boundary 1)

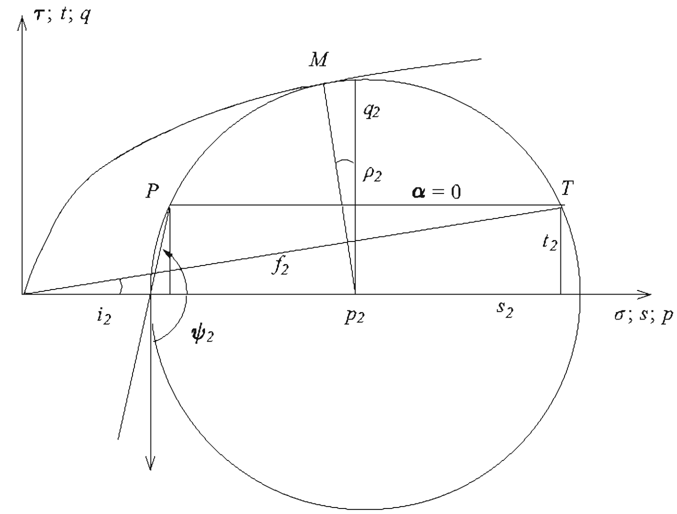

Fig. 6. Mohr's circle for the stress state at Boundary 2 (p = Pole; t = Traction on Boundary 2)

α being the slope angle. In addition, $\sin\theta_1 = t_1/q_1$ so that, the summary is,

$$\psi_1 = \frac{\pi}{2} + \frac{1}{2}\sin^{-1}\left(\frac{t_1}{q_1}\right) - \alpha \tag{27}$$

where T_1, s_1, and α are data (i.e., known), and q_1 is the semi-deviatoric Lambe's variable on Boundary 1 that is expressed by Eq. (6). (Note that therefore ψ_1 is a function of ρ_1 only.)

Solution on the Foundation Plane (Boundary 2)

Transmission of Information from Boundary 1 to Boundary 2

To obtain the stress conditions on the foundation surface (i.e., on Boundary 2) that lead to bearing capacity failure, information needs to be transmitted from Boundary 1 to Boundary 2. Using Riemann's invariants and Eq. (17), the following is obtained

$$I(\rho_2) = I(\rho_1) + \psi_1 - \psi_2 \tag{28}$$

Inclination of the Major Principal Stress

Similarly, ψ_2 is the angle of the major principal stress on Boundary 2 with the vertical axis. Using the Mohr's circle of the stress state on Boundary 2 (see Fig. 6, for which the construction is analogous—with the obvious differences due to having a stress state acting on a horizontal plane, $\alpha = 0$, and an active stress state instead of a passive one—to that discussed with regard to Fig. 5), ψ_2 can be computed as

$$\psi_2 = -\tan^{-1}\left(\frac{p_2 + q_2 - s_2}{t_2}\right) \tag{29}$$

where p_2 and q_2 are functions of the instantaneous friction angle on Boundary 2, ρ_2 [see Eqs. (9) and (10)], and where s_2 and t_2 are the normal and tangential components of the load (traction) acting on the foundation (with inclination i_2). In other words, Eqs. (28) and (29) can be used to compute the value of ρ_2 (and of ψ_2, which is a function of ρ_2 only) as a function of ρ_1 (for a known value of i_2).

The load acting on the foundation surface (i.e., on Boundary 2) can be computed by particularizing Eq. (25) for Boundary 2. The following is obtained:

$$f_2 = \beta_0\left(\frac{n}{\tan\rho_2}\right)^{\frac{1}{1-n}} \times \left[\left(1 + \frac{\tan^2\rho_2}{n}\right)\cos i_2 + \frac{\tan\rho_2}{n\cos\rho_2}\sqrt{1 - \left(\frac{n + (1-n)\sin^2\rho_2}{\sin\rho_2}\right)^2 \sin^2 i_2}\right] \tag{30}$$

Bearing Capacity Factors (or Functions)

Once f_2 is computed using Eq. (30), the bearing capacity can be computed as the normal component, s_2, of the external load, f_2, acting on the foundation (i.e., on Boundary 2) with inclination angle i_2. That is,

$$p_h \equiv s_2 = f_2 \cos i_2 \tag{31}$$

In practice, it is convenient to use a bearing capacity factor, N_β, that, in this case, can be defined as

$$p_h = \beta_0 N_\beta \tag{32}$$

From Eq. (31), N_β for the power-law failure criterion considered herein becomes

$$N_\beta \equiv f_2^* \cos i_2 = \frac{f_2}{\beta_0}\cos i_2 \tag{33}$$

where f_2 is computed from Eq. (30).

For a given soil (i.e., n value) and for a given inclination of the tractions at the foundation (i_2), N_β is exclusively a function of the instantaneous friction angle at Boundary 2, ρ_2. (Because ρ_2 is a function of the magnitude and inclination of tractions applied on Boundary 1, the N_β values are really functions of the tractions on Boundary 1; however, to maintain the traditional geotechnical terminology, the authors prefer to use the term factors to refer to N_β.)

Consideration of Soil's Unit Weight

For strip footings on materials with weight, the contribution of the soil's weight to the bearing capacity is traditionally expressed by $1/2\gamma B N_\gamma S_\gamma$, where γ is the unit weight of the soil (using the submerged unit weight if below the water table), B is the foundation width, N_γ is a bearing capacity factor, and S_γ is a modification factor computed as a product of correction factors that account for foundation shape, inclined loading, foundation depth, surface slope, or base inclination (e.g., Becker and Moore 2006).

In addition to in situ, laboratory, and centrifuge tests, researchers have often employed numerical methods to compute N_γ (e.g., Ueno et al. 2001; Spasojevic and Cabarkapa 2012; Zhu et al. 2001; Lau and Bolton 2011; Kumar and Khatri 2008), and $N_\gamma - \phi$ relationships have been proposed for constant ϕ materials (e.g., Spasojevic and Cabarkapa 2012). Numerical and experimental results show that N_γ generally decreases with foundation size, B and a log–log relationship between them has often been suggested (e.g., Graham and Hovan 1986; Zhu et al. 2001; Kumar and Khatri 2008; Ueno et al. 2001).

To consider the strength nonlinearity in N_γ estimations, one can consider an equivalent (or mobilized) friction angle. For instance, in their numerical limit-analysis approach with a nonlinear failure criterion, Kumar and Khatri (2008) concluded that "a reasonable estimate of N_γ can be obtained even by means of conventional theories [i.e., without considering variations of ϕ with stress level] if an equivalent value of ϕ, as proposed by De Beer (1970), is used."

Zhu et al. (2001) used De Beer's formula (De Beer 1970) to compute secant mobilized friction angles as the size of footings increased, showing that for relatively large footings (say, $B > 4 - 5$ m) the mobilized secant friction angle was only slightly higher (say, $2 - 3°$) than the minimum. Lau and Bolton (2011) used the method of characteristics and Bolton's failure criterion to numerically compute the bearing capacity of circular footings. They showed that, for large footings (say, $B \geq 5$ m), the mean-mobilized secant friction angle is close to the minimum value that corresponds to the highly stressed region below the footing. (In their example, there is approximately a 3° difference between the minimum and the equivalent secant friction angles.) More recently, Spasojevic and Cabarkapa (2012) used Maksimovic's failure criterion to compute bearing capacity factors of a strip footing on sand. Their results also show that the mobilized secant friction angle depends on foundation size, so that N_γ can be computed using the maximum secant friction angle (corresponding to low stresses) for very small foundations, and the minimum (corresponding to high stresses) for very large foundations. Their results also suggest that, for relatively large foundations (say, $B > 5$ m) on silts or sands, the equivalent secant friction angle to compute N_γ is about $3 - 6°$ higher than the minimum.

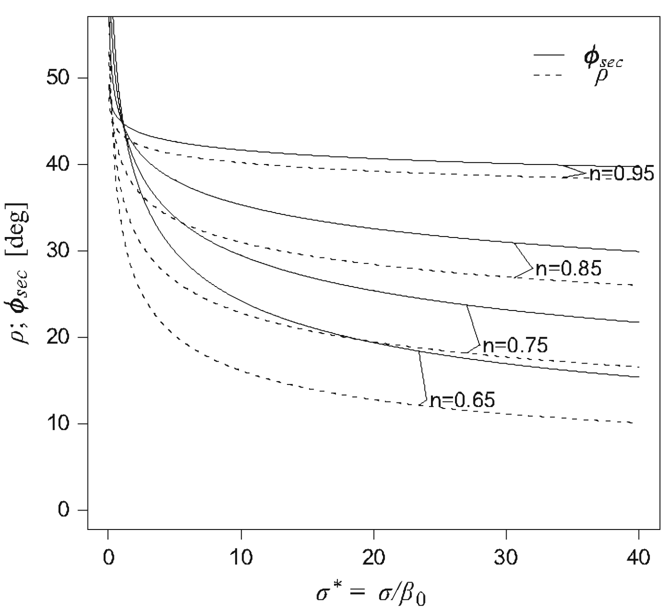

Fig. 7. Relationship between tangent and secant friction angles for different shapes of the failure criterion

The analytical method used here directly provides the minimum and maximum instantaneous (i.e., tangent) friction angles, ρ_2 and ρ_1, that correspond to the areas with higher and lower stresses (respectively, below the foundation and at the free surface). The equivalent tangent friction angle will be intermediate between ρ_1 and ρ_2, and its (minimum) value given by ρ_2 will provide conservative N_γ estimates. But, such obvious lower-bound estimates can be improved. To that end, Fig. 7 compares tangent and secant friction angles for different values of n; as is shown below, differences in Fig. 7 can be employed to better represent friction angles for estimation of N_γ.

Application Examples

Continuous Footing on a Rockfill Slope Edge

Next, a worked example corresponding to a continuous footing located on the edge of a rockfill embankment is presented. The footing transmits a load that is inclined toward the slope, with an angle $i_2 = -10°$. The external slope of the embankment (Boundary 1) is inclined with $\alpha = 10°$, and there is a (vertical) external load applied on the slope with magnitude $f_1 = 200$ kPa and angle $i_1 = -10°$ (see Fig. 1).

Imagine that five rockfill samples have been tested for shear at different normal stress levels, producing the results listed in Table 1. From such values, a linear least-squares fit can be performed [note that Eq. (1) becomes linear after taking the corresponding logarithms]; the result is a model of the form $\tau/\beta_0 = (\sigma/\beta_0)^n$, where $n = 0.864$ and $\beta_0 = 940.5$ kPa. Similarly, a linear fit to compute equivalent MC parameters provides a cohesion intercept of $c = 55.2$ kPa and a friction angle of $\phi = 43.8°$ ($\tan\phi = 0.96$). Fig. 8 shows both fitted failure criteria —power law and MC with a cohesion intercept—and the original rockfill strength data.

Once the power-law strength criterion is fitted, the analytical methodology presented above can be used to compute the bearing capacity of the foundation. The procedure is as follows.

Solution on Boundary 1

1. Given that $f_1 = 200$ kPa, ρ_1 can be computed to satisfy Eq. (26), with the result $\rho_1 = 0.775$ (44.4°).
2. Once ρ_1 is known, Eq. (27) provides the angle of inclination of the major principal stress, ψ_1, with the result $\psi_1 = 1.367$ (78.3°).

Table 1. Rockfill Shear Test Results

σ (kPa)	τ (kPa)
100	135
200	245
400	465
600	635
800	805

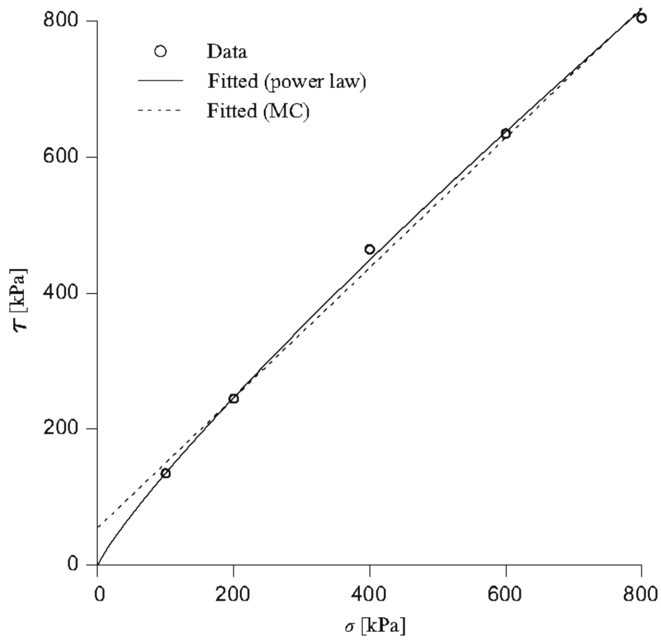

Fig. 8. Fitted failure criteria for the rockfill strength data

Transmission of Information to Boundary 2

1. Using Eq. (22), Riemann's invariant for the computed value of ρ_1 is $I(\rho_1) = 3.63$. The sum of $I(\rho_1) + \psi_1$ is 5.00.

Solution on Boundary 2

1. We get from Eq. (17), it is known that $I(\rho_2) + \psi_2 = 5.00$. Because both $I(\cdot)$ and ψ_2 are functions of ρ_2 only [Eqs. (22) and (29)], ρ_2 is the root of a one-dimensional equation; such computation can be easily performed by iterations or using any standard program for mathematical analysis. In this case, $\rho_2 = 0.618$ (35.4°).
2. Using ρ_2, a value of $f_2 = 9924.5$ kPa is obtained using Eq. (30), from which $N_\beta = 10.39$ using Eq. (33). The bearing capacity is obtained as $p_h = \beta_0 \cdot N_\beta$, and 9775 kPa. $p_h = 9773.75 \approx 9775$ kPa.

(The reader should note that N_β could also be estimated using the design plots discussed below.)

To validate these results with previous methods, the computed bearing capacity can be compared with that obtained with the contributions of the cohesion, c, and external load, q, terms of traditional bearing capacity formulas for MC (c, ϕ) soils (i.e., cN_cS_c and qN_qS_q). (N_c and N_q are bearing capacity factors depending on the soil's friction angle; and S_c and S_q are modification factors that depend on the same aspects as S_γ.) For reference, in the validation the formulas proposed in Sections 10.2.3 and 10.2.4 of the *Canadian Foundation Engineering Manual*, 4th Ed. are used (Becker and Moore 2006). The bearing capacity factors are (considering a rough interface and the errata-corrected formula for N_γ): $N_q = \tan^2(45 + \phi/2)\ \exp(\pi \tan\phi)$, $N_c = (N_q - 1)/\tan\phi$ and $N_\gamma \approx\ 0.1054\exp(0.1675\phi)$; Similarly, the modification factors affecting the example presented here—those due to inclined loading and surface slope—become $s_{qi} = (1 - \tan|i_2|)^2$, $s_{ci} = s_{qi} - (1 - s_{qi})/(N_c \tan\phi)$, and $s_{\gamma i} = (1 - \tan|i_2|)^3$ to correct for inclined loading (the adhesion at the footing's base is neglected); and $s_{q\beta} = s_{\gamma\beta} = (1 - \tan\alpha)^2$, and $s_{c\beta} = s_{q\beta} - (1 - s_{q\beta})/(N_c \tan\phi)$ to correct for sloping ground.

Considering the equivalent MC criterion to the data plotted in Fig. 8 (i.e., $c = 55.2$ kPa and $\phi = 43.8°$), and the geometry of this example ($\alpha = 10°$, $i_2 = -10°$), $N_q = 112.34$ and $N_c = 115.98$

Table 2. Variation of Bearing Capacity Factor N_β for Different Values of α, i_1, and i_2

Case	α (deg)	i_1 (deg)	i_2 (deg)	N_β	Difference (%)
1a	0	0	0	20.29	0
1b	0	10	0	20.89	2.96
1c	0	−10	0	19.27	−5.03
2a	0	0	−10	14.11	−30.46
2b	0	10	−10	14.54	−28.34
2c	0	−10	−10	13.38	−34.06
3a	10	0	0	15.89	−21.69
3b	10	10	0	16.38	−19.27
3c	10	−10	0	15.06	−25.78
4a	10	0	−10	10.98	−45.88
4b	10	10	−10	11.32	−44.21
4c	10	−10	−10	10.39	−48.79

results. Similarly, the modification factors are all approximately equal ($s_{qi} \approx s_{q\beta} \approx s_{ci} \approx s_{c\beta} \approx 0.68$), so that the contribution of the cohesive plus external load terms on bearing capacity is $p_h = 200 \cdot 112.34 \cdot 0.68 \cdot 0.68 + 55.2 \cdot 115.98 \cdot 0.68 \cdot 0.68 \approx 13350$ kPa. Note that this value is significantly (about 35%) larger than the value of p_h computed with our method and the power-law criterion. The reason is that the fitting of the MC envelope did not consider the stress state, whereas our method considers the stress state—and the corresponding instantaneous friction angle—corresponding to each soil element at failure. [The importance of the stress level employed obtain MC failure criteria equivalent to other nonlinear criteria is well known in many geotechnical applications; for example, in the context of tunneling and the Hoek–Brown failure criterion, see Jimenez et al. (2008).] As an illustration of the importance of this, the MC criterion can fit using the high-stress range of experimental data presented in Fig. 8; in particular, if only the last three tests are used, a higher cohesive intercept, $c = 125$ kPa, and a lower friction angle, $\phi = 40.4°$ are obtained. These result in $N_q = 67.54$, $N_c = 78.29$, $s_{qi} \approx s_{q\beta} \approx 0.68$, and $s_{ci} \approx s_{c\beta} \approx 0.67$. Therefore, the bearing capacity contribution of cohesion plus external loading becomes $10\,p_h \approx 10640$ kPa resulting in less than a 10% difference with the method used and the power-law criterion.

Finally, the contribution of the soil's unit weight on bearing capacity needs to be considered. In this case, because the analytical method does not consider weight, the same procedure as used for the polynomial bearing capacity formulas can be followed. As an example, referring to the failure criterion in Fig. 8 (with $n = 0.864$ and $\beta_0 = 940.5$ kPa), it is noted that $\rho_2 = 35.4°$ in the area below the footing. Then, from Fig. 7, it can be seen that the difference between the tangent and secant friction angles for this case is about 4°, which results in a (minimum) secant friction angle of $\phi_{2,sec} \approx 39°$ which is similar to the $\phi = 40.4°$ obtained for the MC fit corresponding to the three tests with higher stress.

Therefore, the (minimum) secant friction angle, $\phi_{2,sec}$, can be used to obtain N_γ estimates for foundations of different size. Based on the discussion above, for $B < 5$ m, one could (conservatively) use an equivalent secant friction angle that is about 3° higher than $\phi_{2,sec}$, resulting in $\phi_{equiv,sec} \approx 42$ and $N_\gamma \approx 120$. For larger foundations, such an increase could be reduced as the size of the foundation increases, until it would become negligible for very large foundations (say, $B > 25$ m), resulting in a value of $\phi_{equiv,sec} \approx \phi_{2,sec} \approx 39$, or $N_\gamma \approx 72.42$. (A log–log relationship can be employed to interpolate between these two values.)

For comparison, the MC soil with failure criterion fitted for the whole stress range ($\phi = 43.8°$) would result in $N_\gamma \approx 160$, whereas the MC criterion fitted for higher stresses ($\phi = 40.4°$) results in $N_\gamma \approx 91.5$, thus being within the range computed with the method presented here. To illustrate the order of magnitude of the overall contribution, considering a foundation of $B = 5$ m width ($N_\gamma \approx 120$), and a rockfill with $\gamma = 18$ kN/m^3, the contribution of soil's unit weight to the ultimate bearing capacity of the soil with a power-law failure criterion would be obtained as $1/2\gamma N_\gamma B s_{\gamma i} s_{\gamma\beta} \approx 2050$ kPa (note that $s_{\gamma i} = 0.56$ and $s_{\gamma\beta} = 0.68$); the results with a MC failure criterion would be computed in the same way, and the only difference would be due to differences in the N_γ factor that result from the ϕ angle selected for linearization.

Finally, in addition to the specific example case presented above, sensitivity analyses were conducted with the geometrical parameters (i.e., i_1, i_2, and α) on N_β. Results are listed in Table 2, where the difference (in percentage) with respect to the reference case ($\alpha = i_1 = i_2 = 0$) also has been included. They show that even small variations of the slope angle, α, or of the inclination angle of the foundation load, i_2, can significantly affect bearing capacity; however, similar variations on the inclination of the load applied on the free surface (i.e., i_1 on Boundary 1) do not have much influence.

Model Tests at Low Gravity

Next, the newly proposed methodology is used to analyze the bearing capacity obtained in load tests conducted with model foundations. In particular, a series of results recently published by Kobayashi et al. (2009) (see also Kobayashi et al. 2007), who conducted tests with two different materials (Toyoura sand and FJS-1 lunar soil simulant), are used at two different relative densities ($D_r = 0.6$ and $D_r = 0.9$) and at several gravity levels (ranging between $0g$ and $2g$, where g is the Earth's gravity value).

This study focuses on the results for Toyoura sand, which is a poorly graded sand often used as a standard for laboratory testing in Japan; the reason is that the failure mechanism for the lunar soil simulant seems to be different from the expected general shear failure mechanism composed of an active failure zone plus a transitional zone plus a passive failure zone (which indeed occurs in Toyoura sand). That is, the lunar soil simulant seems to have a local shear failure zone that is not completely considered by our model. In addition, the scatter of the results corresponding to the lunar soil simulant seems to be higher, which significantly increases the uncertainties in the predictions.

The results of triaxial tests conducted by Kobayashi et al. (2009) are presented in Fig. 9, where (assuming associate plasticity) the best-fitting power-law failure criterion for each case has also been included. (One Mohr circle has been included in each case to emphasize the difference between the $p - q$ and $\sigma - \tau$ failure envelope.) Linear strength parameters proposed by Kobayashi et al. (2009) for each soil are reproduced in Table 3. (Tests were conducted with dry soil and, therefore, parameters obtained are effective strength parameters.) The parameters of the fitted power-law criterion (β_0 and n; see Eq. (2)) are also presented in Table 3.

The size of the model footings were 20 mm×50 mm (width×length), and the bearing capacity tests were conducted inside an aircraft with a parabolic flight path to simulate partial gravity fields. In particular, the test results obtained for low-gravity conditions (i.e., $0g$ to $1/6g$) are used, because such low-gravity conditions eliminate the need for N_γ factors that account for the soil's weight.

Kobayashi et al. (2009) showed that the normalized bearing capacity p_h/c is a linear function of the soil governing parameter, $G = (\gamma N_g B)/2c$, where γ is the bulk density of the soil; N_g is the gravitational acceleration level; and B is the footing width. In other words, for constant γ and B, the bearing capacity becomes a linear function of the gravitational level, so that for negligible values of gravity the bearing capacity becomes independent of the soil's unit weight. In particular, for a (linear) $c - \phi$ soil, the bearing capacity would be given by $p_h = c \cdot N_c$.

Table 4 presents the experimental values of bearing capacity for zero-gravity conditions that are inferred from Kobayashi et al. (2009). They were obtained evaluating at $G = 0$, a straight line that is fitted to estimate bearing capacity values over a wider range of G values ($G \in 0.0, 0.25$). Similarly, Table 4 presents the

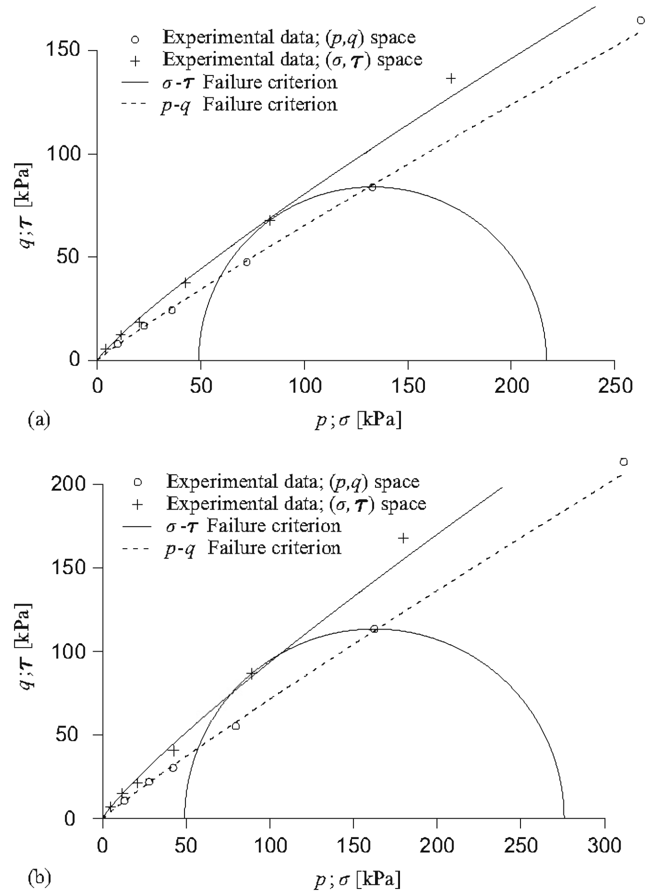

Fig. 9. Testing data and (nonlinear) fitted failure criteria. (a) Toyoura $D_r = 0.6$; (b) Toyoura $D_r = 0.9$

Table 3. Strength Parameters of the Soils Used for the Linear and Power-Law Failure Criteria

Soil	D_r (%)	Linear		Power-law	
		c' (kPa)	ϕ' (deg)	β_0 (kPa)	n
Toyoura	60	3.04	38.1	21.03	0.86
	90	3.04	42.7	61.33	0.86

Table 4. Experimental Results and Analytical Estimations of Bearing Capacity for Zero-Gravity Conditions

Soil	Experimental		Analytical (kPa)	
	p_h/c[a]	p_h (kPa)	Linear p_h	Power-law p_h
Toyoura $D_r = 0.6$	6.3	19.15	138.4	17.3
Toyoura $D_r = 0.9$	13.0	42.26	308.6	48.3

[a]Estimated from linear fit evaluated at $G = 0$.

predictions that would be obtained using typically available analytical methods for bearing capacity estimation of $c-\phi$ soils [e.g., either by Prandtl's formula or by the characteristics method employed by Kobayashi et al. (2009), as both agree in this case], as well as the predictions obtained when the power-law failure criterion is considered with the analytical solutions presented herein. For the predictions of the power-law method, it has to be noted that the foundation is located on the surface and that, therefore, the external load on Boundary 1 is zero (i.e., $f_1 = 0$). This produces numerical difficulties that were already identified by Sokolovskii (1965) (see also Zhu et al. 2001; Graham and Hovan 1986; Ueno et al. 2001; Spasojevic and Cabarkapa 2012), who suggested that the bearing capacity could be estimated from solutions computed using a small value of f_1 and using an estimated slope of the solution at that point. (In this case, bearing capacities for $f_1^* = 0$ conditions were estimated using computed values for $f_1^* = 0.02\%$ and $f_1^* = 0.04\%$.)

Results show that, although the predictions of the power-law model are not perfect (remember that, due to testing difficulties, significant uncertainties and scatter exist in the available experimental results), they significantly improve the analytical predictions of the linear (MC) case, which tend to significantly overpredict the experimental results. This is probably due to the influence of the nonzero cohesion obtained when the linear MC failure criterion is assumed, as such cohesion significantly increases the shear strength of the soil at low values of normal stress.

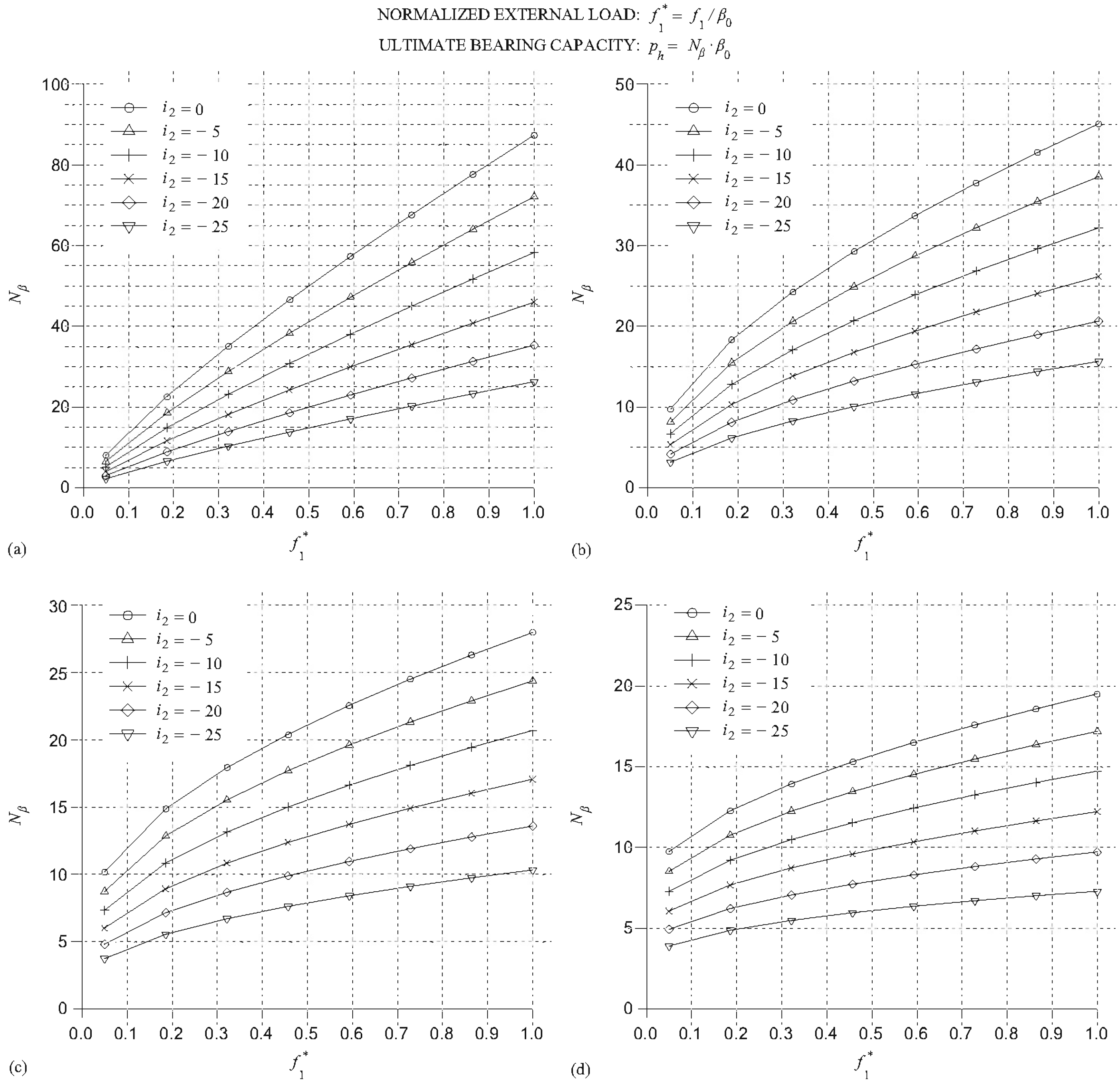

Fig. 10. Plots for simplified computation of the bearing capacity factor for a slope angle $\alpha = 0$: (a) $n = 0.95$; (b) $n = 0.85$; (c) $n = 0.75$; (d) $n = 0.65$

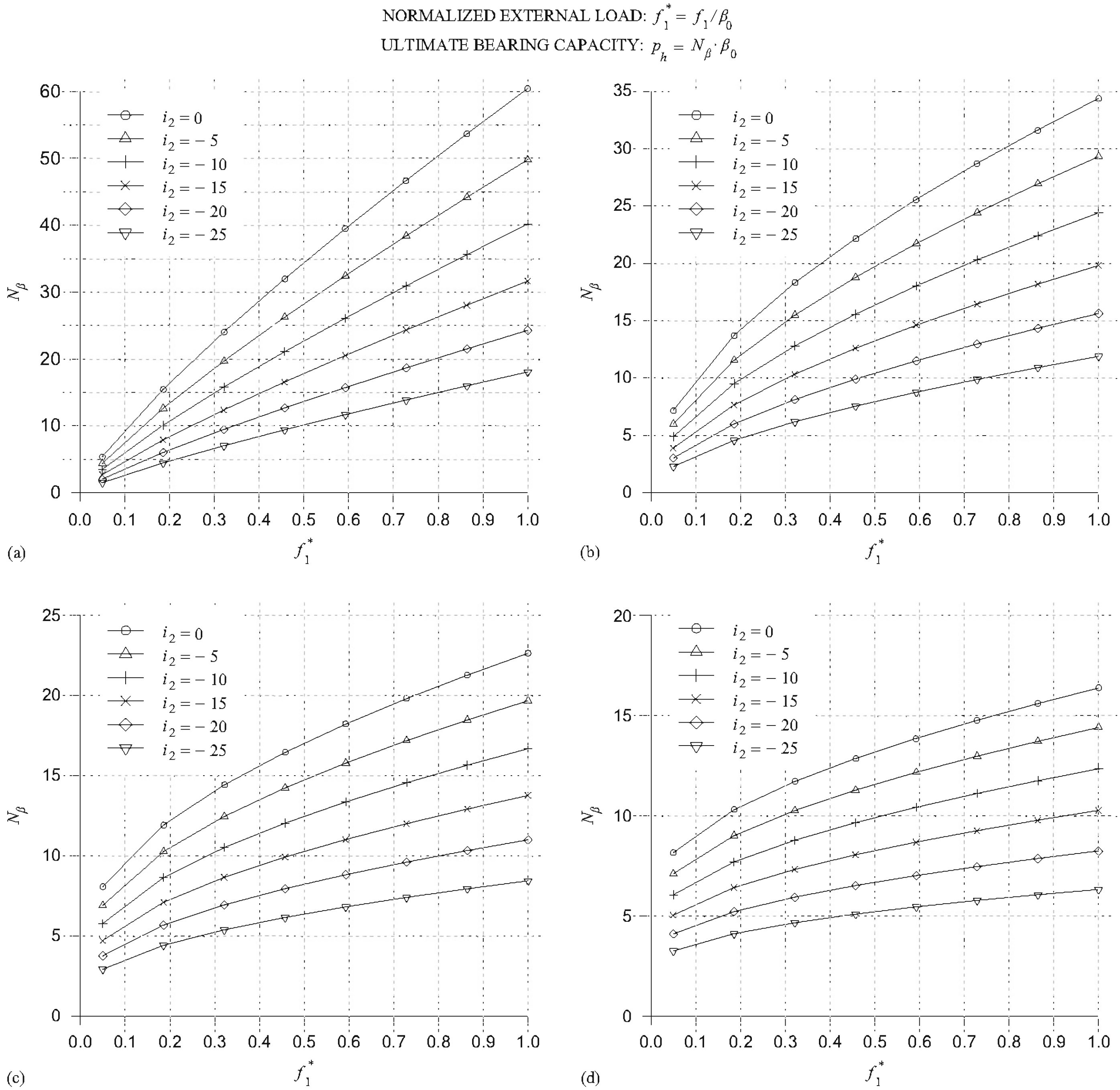

Fig. 11. Plots for simplified computation of the bearing capacity factor for a slope angle $\alpha = 10$: (a) $n = 0.95$; (b) $n = 0.85$; (c) $n = 0.75$; (d) $n = 0.65$

Design Graphs for Approximate Computations

Results presented in Fig. 4 and in Table 2 suggest that inclination of the external load acting on the free surface does not have a significant influence on bearing capacity. Therefore, design plots that allow a direct (and approximate) estimation of N_β can be developed.

In particular, Figs. 10–12 have been developed by considering that the external load on the free surface is vertical (i.e., $i_1 = -\alpha$). They present the bearing capacity factors or functions, N_β, for different values of $n\alpha$, and i_2. (Note that, for ease of generalization, the input external load acting on the free surface are normalized as $f_1^* = f_1/\beta_0$.) Once N_β is obtained, the ultimate bearing capacity can by computed as $p_h = N_\beta \cdot \beta_0$.

Conclusions

In this paper, an analytical solution is presented to compute the bearing capacity, under plane-strain, for materials with a power-law failure criterion. The solution is obtained using the method of characteristics, considering the magnitude and orientation of tractions at the free surface and below the foundation. The new solution is quite general, and its implementation is simple.

The contribution of the soil's self-weight on bearing capacity is not considered in the analytical solution presented, but it can be incorporated in the analysis using the traditional N_γ factors. A worked case example is presented in detail, and the procedure to select approximate (or conservative) friction angles to estimate N_γ is discussed.

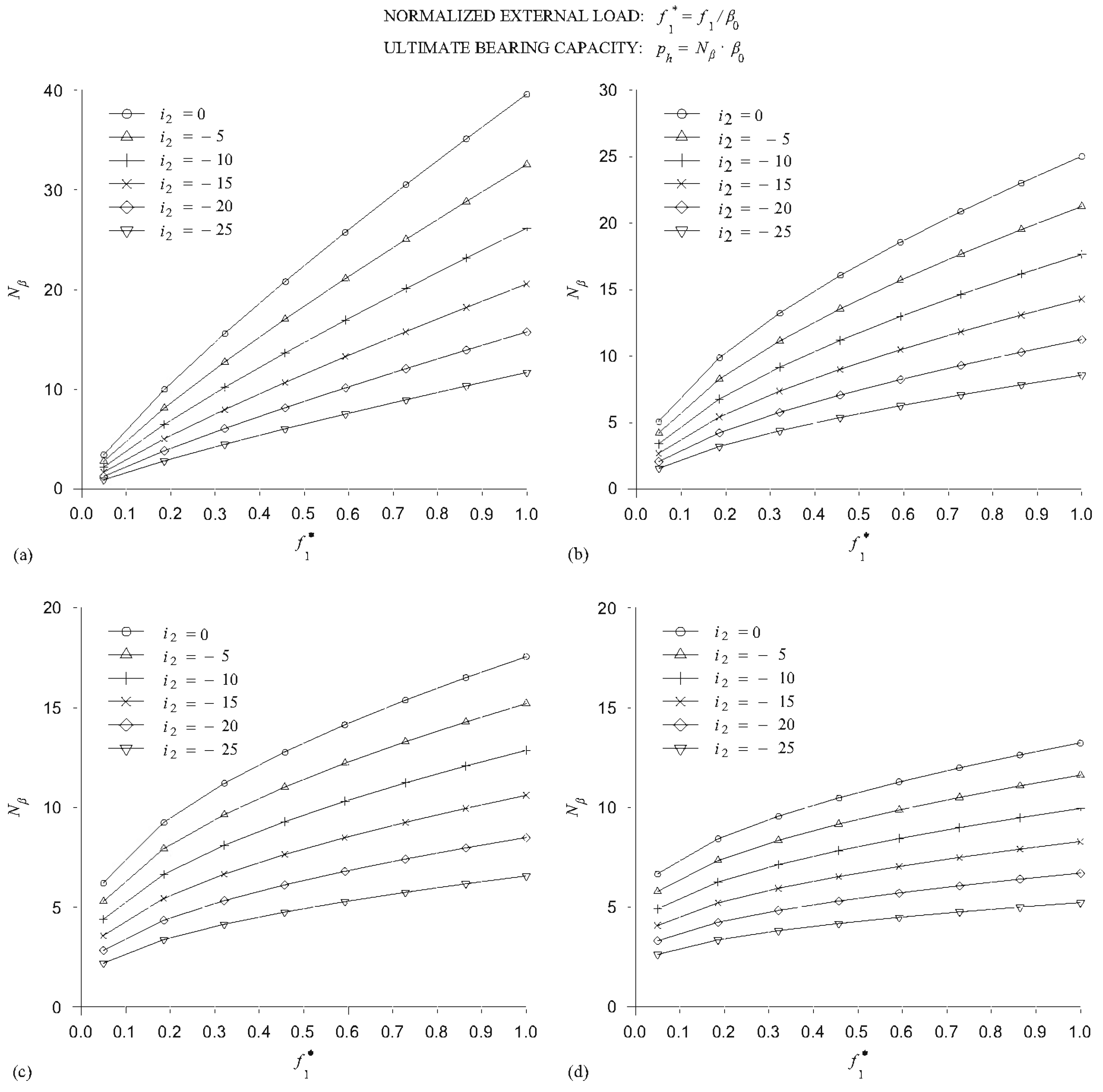

Fig. 12. Plots for simplified computation of the bearing capacity factor for a slope angle $\alpha = 20$: (a) $n = 0.95$; (b) $n = 0.85$; (c) $n = 0.75$; (d) $n = 0.65$

Results from a sensitivity analysis are presented, as well. They suggest that the magnitude of the external surcharge on the free surface, as well as the inclination of the foundation load, strongly affect bearing capacity; the slope angle is also important, whereas the inclination of the external surcharge has a more limited influence. This has allowed the authors to present design plots for fast and simple (although approximate) bearing capacity estimations.

Finally, the model has been employed to verify the results of bearing capacity tests conducted under conditions of low gravity. Results suggest that the newly proposed method improves traditional bearing capacity estimates based on a linear failure criterion.

Appendix: Convergence of Solutions to the Linear Case (i.e., $n = 1$) Load Factors

Next, it is verified that the bearing capacity factors computed herein converge toward traditional solutions for the limiting case of $n = 1$ (i.e., for the linear case). The check will be conducted for the case of horizontal surfaces and vertical loads (i.e., $i_1 = i_2 = \alpha$).

For Boundary 1, the external load acting on the free surface is given by $q_e \equiv s_1 = \sigma_{III,1}$, where $\sigma_{III,1}$ is the minor principal stress acting on Boundary 1, and

$$q_e \equiv \sigma_{III,1} = \frac{\sigma_1}{1 + \sin\rho_1}\left[1 - \left(\frac{1-n}{n}\sin\rho_1\right)\right] \tag{34}$$

For Boundary 2, the ultimate (failure) load corresponds to the major principal stress, so that $p_h \equiv s_2 = \sigma_{I,2}$, and

$$p_h \equiv \sigma_{I,2} = \frac{\sigma_2}{1 - \sin \rho_2}\left[1 + \left(\frac{1-n}{n} \sin \rho_2\right)\right] \tag{35}$$

Define the ratio $N_{qg} \equiv p_h / q_e$, which is a generalization of Prandtl's coefficient N_q, $p_h = q_e N_{qg}$. For the power-law failure criterion considered herein, using Eqs. (34) and (35),

$$N_{qg} \equiv \frac{p_h}{q_e} = \left(\frac{1+\sin\rho_2}{1-\sin\rho_1}\right)\left(\frac{\sigma_2}{\sigma_1}\right)\left(\frac{n+(1-n)\sin\rho_2}{n-(1-n)\sin\rho_1}\right) \tag{36}$$

and, using Eq. (4),

$$N_{qg} \equiv \frac{p_h}{q_e} = \left(\frac{1+\sin\rho_2}{1-\sin\rho_1}\right)\left(\frac{\tan\rho_1}{\tan\rho_2}\right)^{\frac{1}{1-n}}\left(\frac{n+(1-n)\sin\rho_2}{n-(1-n)\sin\rho_1}\right)$$
$$= F_1 \cdot F_2 \cdot F_3, \tag{37}$$

where F_1, F_2, and F_3 are functions of the instantaneous friction angles.

In the linear case ($n = 1$), the instantaneous friction angle is constant, and the failure criterion can be expressed with a (constant) parameter, ϕ. Then, it can be demonstrated that coefficient N_{qg} converges to Prandtl's coefficient N_q as ρ_1 and ρ_2 tend to ϕ. The limit of N_{qg} can be computed as the product of the limits of three terms with finite limits that are nonzero. For n tending to one (i.e., $n \to 1$), and considering that the instantaneous friction angles ρ_1 and ρ_2 are linked by Eq. (17),

$$\begin{aligned}\lim N_{qg} &= \lim F_1 \cdot \lim F_2 \cdot \lim F_3 = \\ &= \tan^2(\pi/4 + \rho_1/2) \cdot \exp(\pi \tan \rho_1) \cdot 1 = \\ &= N_q(\rho_1) = N_q(\phi)\end{aligned} \tag{38}$$

which is the classical N_q expression for materials with a linear failure criterion that was presented by Prandtl in 1920. [Lau and Bolton (2011) also derived this equation for weightless frictional soils linking the rotation of principal stress directions and the associated change of their magnitude.]

Acknowledgments

Professor Taizo Kobayashi, of University of Fukui (Japan), provided the original testing data for the Toyoura sand employed in their low-gravity model foundation tests. His support is kindly acknowledged.

References

Anyaegbunam, A. J. (2013). "Nonlinear power-type failure laws for geomaterials: Synthesis from triaxial data, properties and applications." *Int. J. Geomech.*, 10.1061/(ASCE)GM.1943-5622.0000348, 04014036.

Baker, R. (2004). "Nonlinear Mohr envelopes based on triaxial data." *J. Geotech. Geoenviron. Eng.*, 10.1061/(ASCE)1090-0241(2004)130:5(498), 498–506.

Baker, R., and Frydman, S. (1983). "Upper bound limit analysis of soil with non-linear failure criterion." *Soils Found.*, 23(4), 34–42.

Becker, D. E., and Moore, I. D., eds. (2006). *Canadian Foundation Engineering Manual*, 4th Ed., Canadian Geotechnical Society, Richmond, BC, Canada.

Bishop, A. W. (1966). "The strength of soils as engineering materials." *Geotechnique*, 16(2), 89–130.

Bolton, M. D. (1986). "The strength and dilatancy of sands." *Geotechnique*, 36(1), 65–78.

Bolton, M. D., and Lau, C. K. (1993). "Vertical bearing capacity factors for circular strip footings on Mohr-Coulomb soil." *Can. Geotech. J.*, 30(4), 1024–1033.

Brinch-Hansen, J. (1961). *A general formula for bearing capacity*, Bull. No. 11, Danish Geotechnical Institute, Copenhagen.

Charles, J. A., and Watts, K. S. (1980). "The influence of confining pressure on the shear strength of compacted rockfill." *Geotechnique*, 30(4), 353–367.

Chen, W. F. (1975). *Limit analysis and soil plasticity*, Elsevier, Amsterdam.

De Beer, E. E. (1970). "Experimental determination of the shape factors and bearing capacity factors for sand." *Geotechnique*, 20(4), 387–411.

Drescher, A., and Detournay, E. (1993). "Limit load in translational failure mechanisms for associative and non-associative materials." *Geotechnique*, 43(3), 443–456.

Graham, J., and Hovan, J.-M. (1986). "Stress characteristics for bearing capacity in sand using a critical state model." *Can. J. Geotech. Eng.*, 23(2), 195–202.

Indraratna, B., Wijewardena, L., and Balasubramanian, A. N. (1993). "Large-scale triaxial testing of greywacke rockfill." *Geotechnique*, 43(1), 37–51.

Jimenez, R., Serrano, A., and Olalla, C. (2008). "Linearization of the Hoek and Brown rock failure criterion for tunnelling in elasto-plastic rock masses." *Int. J. Rock Mech. Mining Sci.*, 45(7), 1153–1163.

Ko, H. Y., and Scott, R. F. (1973). "Bearing capacities by plasticity theory." *J. Soils Mech. Found. Div. ASCE*, 99(SM-1), 1–23.

Kobayashi, T., Ochiai, H., Suyama, Y., Aoki, S., Yasufuku, N., and Omine, K. (2009). "Bearing capacity of shallow foundations in a low gravity environment." *Soils Found.*, 49(1), 115–134.

Kobayashi, T., Ochiai, H., and Yasufuku, N. (2007). "Mechanical properties and bearing capacity of lunar surface," *Proc., 13th Asian Regional Conference on Soils Mechanics and Geotechnical Engineering*, Vol. 1, Kolkata, India, 149–152.

Kumar, J., and Khatri, V. N. (2008). "Effect of footing width on n_γ." *Can. Geotech. J.*, 45(12), 1673–1684.

Lau, C. K., and Bolton, M. D. (2011). "The bearing capacity of footings on granular soils. I: Numerical analysis." *Geotechnique*, 61(8), 627–638.

Lyamin, A. V., and Sloan, S. W. (2002a). "Lower bound limit analysis using non-linear programming." *Int. J. Numer. Meth. Eng.*, 55(5), 573–611.

Lyamin, A. V., and Sloan, S. W. (2002b). "Upper bound limit analysis using linear finite elements and non-linear programming." *Int. J. Numer. Anal. Meth. Geomech.*, 26(2), 181–216.

Maeda, K., and Miura, K. (1999). "Confining stress dependency of mechanical properties of sands." *Soils Found.*, 39(1), 53–67.

Maksimovic, M. (1989). "Nonlinear failure envelope for soils." *J. Geotech. Geoenviron. Eng.*, 10.1061/(ASCE)0733-9410(1989)115:4(581), 581–586.

Maksimovic, M. (1996). "A family of nonlinear failure envelopes for non-cemented soils and rock discontinuities." *Electron. J. Geotech. Eng.*, 1(1), 1–36.

Meyerhof, G. G. (1951). "The ultimate bearing capacity of foundations." *Geotechnique*, 2(4), 301–332.

Michalowski, L. (1997). "An estimate of the influence of soil weight on bearing capacity using limit analysis." *Soils Found.*, 37(4), 57–64.

Mitchell, J. K., and Soga, K. (2005). *Fundamentals of soil behavior*, 3rd Ed., John Wiley & Sons,Hoboken, NJ.

Pope, R. G. (1975). "Non-dimensional chart for the ultimate bearing capacity of surface and shallow foundations." *Geotechnique*, 25(3), 593–597.

Serrano, A., and Olalla, C. (1994). "Ultimate bearing capacity of rock masses." *Int. J. Rock Mech. Mining Sci. Geomech. Abstr.*, 31(2), 93–106.

Serrano, A., and Olalla, C. (2006). "Discussion of 'Nonlinear Mohr envelopes based on triaxial data' by R. Baker." *J. Geotech. Geoenviron. Eng.*, 10.1061/(ASCE)1090-0241(2006)132:1(128.3), 128–130.

Serrano, A. A. (1976). *Geotecnia y Cimientos II: Soils and Rock Mechanics*, Vol. II. Editorial Rueda, Madrid.

Sokolovskii, V. V. (1965). *Statics of granular media*, Pergamon Press Limited, London.

Spasojevic, A., and Cabarkapa, Z. (2012). "Extended stress field analysis of surface strip footing on sand." *Geotechnique*, 62(8), 733–740.

Terzaghi, K. (1943). *Theoretical soil mechanics*, John Wiley & Sons, New York.

Ueno, K., Miura, K., Kusakabe, O., and Nishimura, M. (2001). "Reappraisal of size effect of bearing capacity from plastic solution." *J. Geotech. Geoenviron. Eng.*, 10.1061/(ASCE)1090-0241(2001)127:3(275), 275–281.

Ukritchon, B., Whittle, A. J., and Sloan, S. W. (1998). "Undrained limit analysis for combined loading of strip footings on clay." *J. Geotech. Geoenviron. Eng.*, 10.1061/(ASCE)1090-0241(1998)124:3(265), 265–276.

Vesic, A. S. (1975). *Foundation engineering handbook*, Reinhold, New York.

Zhu, F., Clark, J. I., and Phillips, R. (2001). "Scale effect of strip and circular footings resting on dense sand." *J. Geotech. Geoenviron. Eng.*, 10.1061/(ASCE)1090-0241(2001)127:7(613), 613–621.